The Dynamics of Thermal-Induced Phase Separation in PMMA Solutions

P. D. Graham, A. J. Pervan, and A. J. McHugh*

Department of Chemical Engineering, University of Illinois, 600 South Mathews, Urbana, Illinois 61801

Received November 22, 1996; Revised Manuscript Received January 23, 1997[⊗]

ABSTRACT: Small-angle light scattering and scanning electron microscopy (SEM) have been used to study morphology development in poly(methyl methacrylate) membranes formed by the thermal inversion method. Analysis of the early time behavior of the scattered intensity in terms of Cahn−Hilliard theory establishes spinodal decomposition as the mechanism of phase separation for the conditions studied. The intensity maximum position for late-stage growth follows a power law dependence with a time exponent of approximately one-third, which is consistent with diffusive coarsening mechanisms. Solutions quenched to regions of the phase diagram below the glass transition temperature show an immediate arrest in the location of the scattered intensity maximum, indicating a locking-in of the phase-separated structure. Domain sizes obtained from SEM measurements of annealed, quenched samples are shown to be consistent with light scattering measurements.

Introduction

Thermal-induced phase separation (TIPS) has been shown to be an excellent way to make microporous polymeric membranes.[1−4] In this process, a homogenous polymer solution is cooled to a temperature below the binodal line, where the solution phase separates into a polymer-rich phase and a polymer-lean phase. Phase separation continues until the polymer-rich phase becomes immobilized by gelation, glass transition, or crystallization. Once this occurs, the structure is effectively frozen into place and the solvent can be removed from the film. The dried film can then serve as a microporous membrane. The morphology of the film determines the separation power of the membrane, and therefore, its control is crucial to the production of useful membranes.

Membrane morphology is controlled by the mechanism of the initial phase separation, the kinetics of domain growth following phase separation, and the exact way in which the solidification process interrupts domain growth. Light scattering has been used extensively to study both the initial phase separation process and the subsequent late-stage coarsening in many polymer solutions.[5−11] Many of these studies have shown that spinodal decomposition plays an important role in off-critical quenches and that late-stage coarsening is often faster than that predicted by diffusive coarsening mechanisms. Several studies have shown that late-stage coarsening can be monitored using real space microscopy.[12−16] While reports of initial phase separation and late-stage coarsening abound, studies that show the cessation of domain growth by solidification are quite scarce. Bansil et al.[7] used light scattering to show how late-stage coarsening can be interrupted by gelation in a swine skin gelatin solution; however, there have been no studies reported that directly examine the vitrification process in membrane-forming systems.

This paper presents the results of an investigation of the initial phase separation process, the kinetics of domain growth, and the cessation of domain growth by solidification and their role in the morphological development of membranes made from poly(methyl methacrylate) (PMMA)/cyclohexanol solutions. Analysis of the time progression and the angular distribution of scattered light is used to establish the phase separation mechanism. Late-stage coarsening behavior is studied both by monitoring the progression of the scattering maximum and by analyzing scanning electron micrographs of membranes allowed to coarsen for different amounts of time. The results of the scattering measurements and the real space analysis show good quantitative agreement. The light-scattering experiments also show that glass transition locks in certain morphologies in membrane-forming systems.

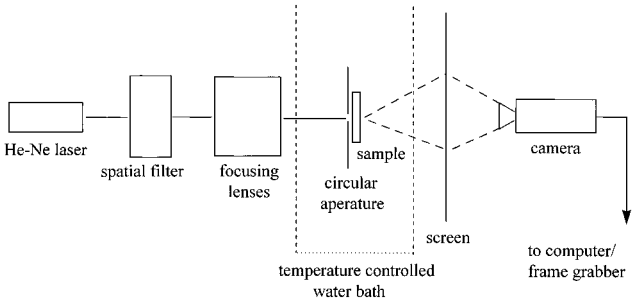

Figure 1. Schematic of the SALS apparatus.

Experimental Section

Atactic PMMA ($M_w \sim 15\,000$) was purchased from Aldrich. Solutions made from the as-received polymer appeared cloudy, indicating the presence of an impurity. To remove the impurity, solutions of PMMA in dichloromethane were centrifuged, the clear top layer was decanted, and the solvent was allowed to evaporate. Reagent grade cyclohexanol (Aldrich) was used as received.

The cloud point curve was determined by making PMMA/cyclohexanol solutions of several different compositions. Solutions were placed into test tubes (diameter 0.5 cm) and annealed to ensure sample uniformity before being cooled at a rate of 0.5 °C/minute. The cloud point was taken as the temperature at which the sample became opaque. Reproducibility of the cloud point measurements was within ± 0.1 °C.

Figure 1 shows a schematic of the small-angle light-scattering (SALS) apparatus. The incident beam (10 mW He−Ne laser) passes through a spatial filter to increase beam

[⊗] Abstract published in *Advance ACS Abstracts,* March 1, 1997.

S0024-9297(96)01720-2 CCC: $14.00

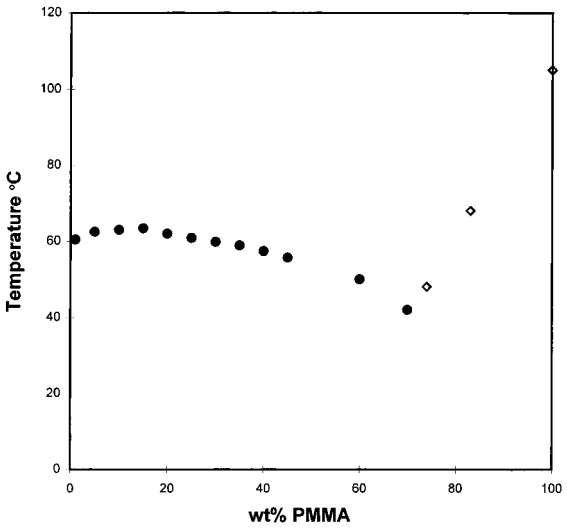

Figure 2. Cloud point curve (●) and glass transition curve (◇) (from Vandeweerdt et al.[18]) for PMMA/cyclohexanol system.

homogeneity before being focused to a diameter of ~1 mm. The circular aperture just prior to the sample is used to eliminate parasitic scattering. Scattered light from the sample falls onto an opal glass viewing screen, and the resultant pattern is recorded by a video camera and digitized by a frame grabber card.

Samples used for the light-scattering experiments were prepared by first applying an epoxy adhesive around the perimeter of a large (50 mm × 75 mm) microscope slide. A small amount of PMMA/cyclohexanol solution was placed in the center of the slide and a second slide, used to cover the solution, was pressed firmly into place. Care was taken to avoid bubbles during the casting procedure. Samples prepared in this way had thicknesses of ~0.2 mm.

Samples used for scanning electron microscopy (SEM) analysis were prepared by placing PMMA/cyclohexanol solutions into clear glass vials (diameter 0.5 cm). Before performing any membrane-casting experiments, the cloud point of all of the samples was measured. Some of the samples had a cloud point that was lower than the rest. The hygroscopic nature of cyclohexanol is thought to be the cause of this variation. During the loading procedure, small amounts of water may have been absorbed by the solution and slight additions of water are known to drastically lower the cloud point of these solutions.[17] Any sample with a lower cloud point was discarded. The remaining samples were allowed to homogenize at 75 °C before being placed into a temperature-controlled water bath set to the desired phase separation temperature. Samples were allowed to phase separate for differing amounts of time before being quenched in ice/water. Following removal from the test tubes, the samples were fractured to expose their cross sections and vacuum-dried for at least 24 h. Samples were sputter coated (Emscope SC400 Sputter coater) and imaged using a Hitachi S-530 scanning electron microscope.

Results and Discussion

Phase Diagram. Figure 2 shows the cloud point and glass transition curves for the PMMA/cyclohexanol system. The glass transition temperatures are those reported by Vandeweerdt et al.[18] The most important feature of the phase diagram is that the cloud point and the glass transition curves intersect, which implies that there are regions where glass transition can interfere with phase separation. At temperatures in the two-phase region above the intersection point, the solution will separate into a viscous polymer-rich liquid and a much less viscous polymer-lean phase. The mobility of both of the liquid phases is high enough that domain growth will continue until the domains have become quite large. At temperatures below the intersection point, the polymer-rich phase undergoes a glass transition, which can serve to kinetically freeze the morphology.

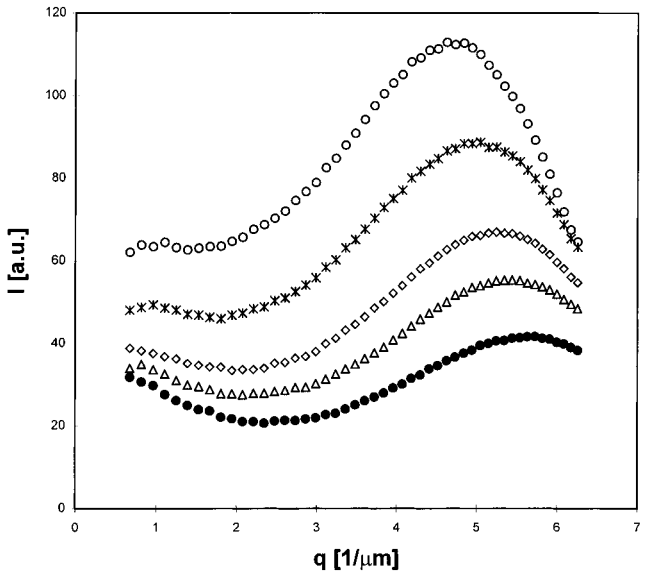

Figure 3. Scattered light intensity vs wavenumber following a quench of a 35 wt % PMMA solution to 50 °C: (●) 10, (△) 20, (◇) 30, (∗) 50, and (○) 100 s.

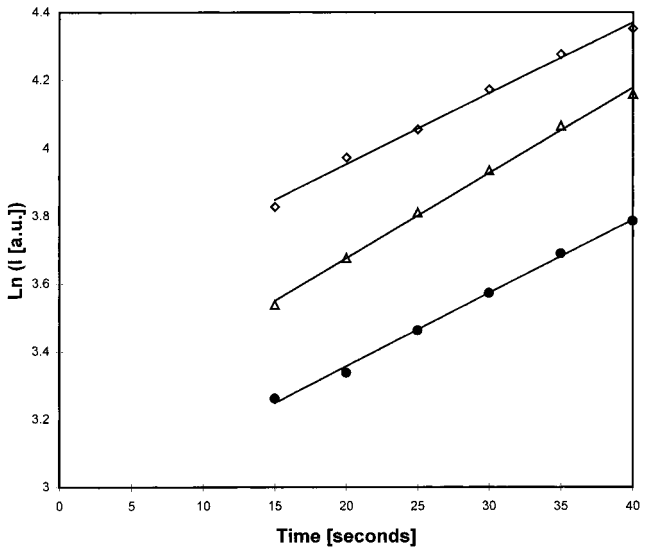

Figure 4. Initial time dependence of scattered intensity at several wavenumbers for 35 wt % solution quenched to 50 °C: (●) 3.36, (Δ) 4.51, and (◇) 5.54 μm^{-1}.

Light Scattering Results. Figure 3 shows the scattered intensity (I) vs wavenumber ($q = 4n\pi/\lambda \sin \theta/2$, where θ is the scattering angle, λ is the wavelength in vacuo, and n is the solution refractive index) at several times for an initially homogenous 35 wt % PMMA/cyclohexanol solution quenched to 50.0 °C. Although the run lasted several hours, only the data for the first few minutes are shown in order to make the early-stage behavior as clear as possible. The presence of a maximum in the I vs q plot and its progressive shift to lower wavenumbers are characteristics of phase separation by spinodal decomposition.[19−21] Standard Cahn−Hilliard analysis[19,20] predicts that the intensity at a given wavenumber should grow exponentially with time. To illustrate this, Figure 4 shows the logarithm

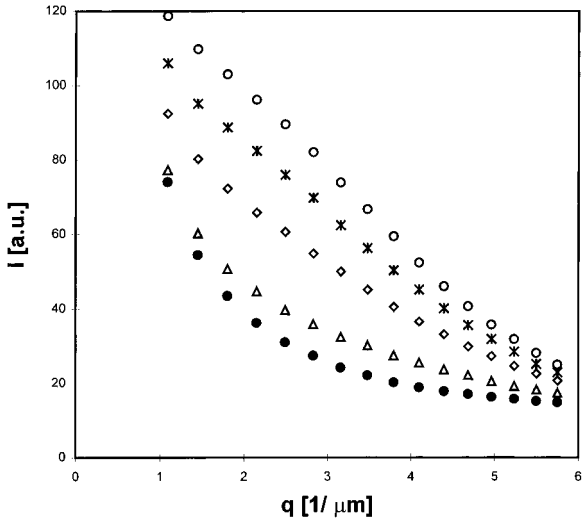

Figure 5. Scattered light intensity vs wavenumber following a quench of a 50 wt % PMMA solution to just below cloud point: (●) 30, (Δ) 90, (◇) 135, (∗) 195, and (○) 315 s.

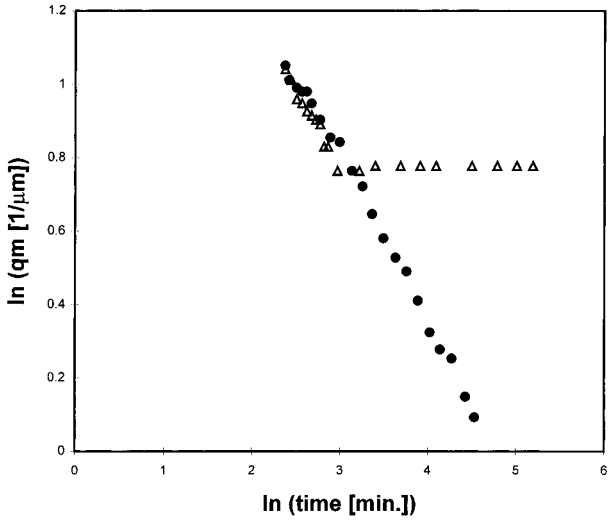

Figure 6. Position of scattering maximum as a function of time for isothermal phase separation at 50 °C (●); and for a quench to 25 °C following 30 min at 50 °C (Δ).

of the intensity plotted vs time for three representative wavenumbers. The excellent fit demonstrates that, for the indicated time scale, spinodal decomposition is the phase separation mechanism.

It should be noted that not all quenches resulted in a scattering pattern with an intensity maximum. For example, Figure 5 shows a plot of I vs q for a 50 wt % solution quenched just below its cloud point. As time proceeds, the intensity of the scattered light increases, but there is never any sign of a maximum. This type of scattering pattern has been seen in previous studies of phase separation in polymer blends[21] and polymer solutions[22] and has been attributed to phase separation by nucleation and growth. In our system, nucleation and growth was only observed to occur in a very small temperature range (undercoolings less than 0.5 °C) for the more concentrated solutions. For this reason, the remainder of this paper discusses exclusively experiments conducted in the spinodal region of the phase diagram.

For later stages of phase separation by spinodal decomposition, the position of the intensity maximum generally obeys a growth law of the form,

$$q_m \propto t^{-\alpha} \tag{1}$$

where q_m is the wavenumber of the intensity maximum and α is the growth exponent. As shown by theoretical considerations[23] and direct experimental evidence,[21,24] q_m can be inversely related to the dominant size scale, D_{ls}, in the phase-separating system,

$$D_{ls} = 2\pi/q_m \tag{2}$$

Therefore, any process that affects the ability of the domains to coarsen should also affect the time progression of the scattering maximum.

To determine whether the value of α is different in regions of the phase diagram where glass transition is important, two separate experiments were conducted. In the first, initially homogenous solutions were quenched to two-phase regions of the phase diagram above the intersection of the cloud point curve and the glass transition curve and held there for the duration of the experiment. The closed symbols in Figure 6 illustrate an example of the time behavior of q_m for a 35 wt % solution that was quenched from 80 to 50 °C. The data are linear with a slope of −0.36, indicating that domains grow with the same time dependence for the entire experiment. The value of the exponent is roughly consistent with diffusive coarsening by either coalescence[25] or Ostwald ripening.[26]

In addition to isothermal phase separation, we also conducted experiments where the solution was allowed to phase separate for a fixed time in a region above the intersection of the cloud point and the glass transition before being rapidly quenched to a region where glass transition can occur. The open symbols in Figure 6 show the results of an experiment in which the 35 wt % solution was allowed to phase separate at 50.0 °C for 30 min before quenching to room temperature. On quenching, the position of the scattering maximum immediately stops moving inward, indicating the arrest of domain growth and consequent locking in of the morphology. To eliminate the possibility that the arrest of domain growth is related to the freezing of the cyclohexanol (melting temperature ∼22 °C) we have conducted experiments that show the structure is locked in by a quench to 35 °C.

Thus, in Figure 6 it is clearly shown that light scattering provides a direct way to probe exact conditions under which phase separation is arrested and certain morphologies are frozen into place. Not only does this process play a crucial role in the morphological development of membranes formed by thermal inversion, but the structures formed by non-solvent-induced phase inversion are also believed to result from a combination of phase separation and vitrification.[27,28]

Combined Light Scattering and Real Space Microscopy. As shown in Figure 6, there is no change in the dominant structure once the samples have been quenched to room temperature. Therefore, samples allowed to phase separate under a variety of conditions can be quenched to room temperature and prepared for SEM observation. These morphologies can then be related to the position of the scattering maximum for a film processed under identical conditions. For example, Figure 7 shows SEM sample cross sections and corresponding light-scattering patterns for a 35 wt % solution allowed to coarsen for three representative time periods at 50 °C. Qualitatively, it is clearly seen that the scattering maximum occurs at smaller angles (smaller

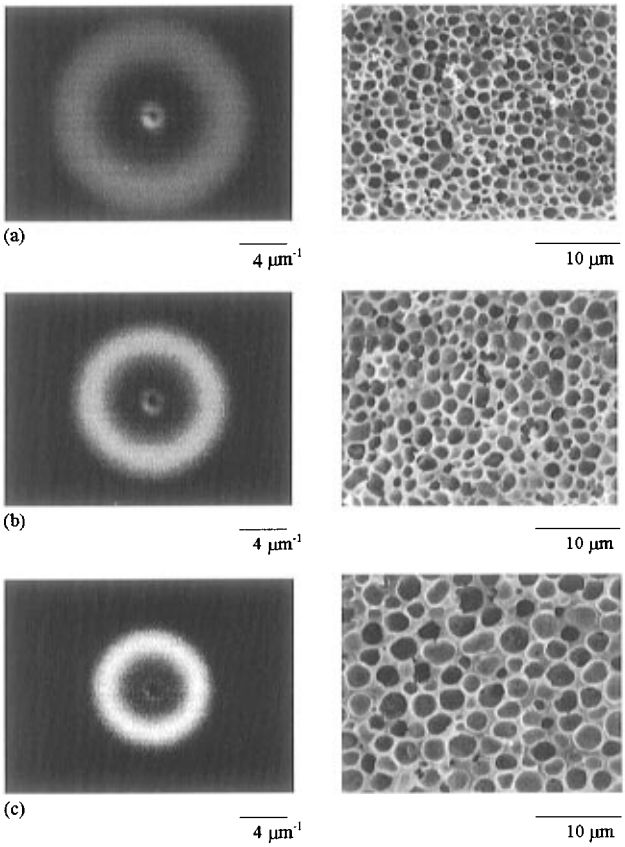

Figure 7. Light scattering patterns and corresponding sample cross sections for several times following quench of a 35 wt % solution to 50 °C: (a) 15, (b) 30, and (c) 60 min.

q) as the morphology coarsens. A limitation of the experimental procedure is that the scattering patterns and real space data are obtained from different samples. Although both samples were prepared from identical solutions, it was nearly impossible to prepare scattering samples and real space samples having exactly the same cloud point. It has been shown that a slight variation in the cloud point can dramatically affect the position of the scattering maximum, without altering the growth exponent.[17] Therefore, a growth rate comparison is valid; however, it is impossible to determine quantitatively a relation between the domain size predicted by light scattering and measured in real space. For this reason, we choose to treat eq 2 as a proportionality between D_{ls} and q_m rather than an equality.

To quantitatively compare the time dependence of the position of the scattering maximum and the domain growth observed in real space, a series of micrographs were analyzed. The domain size is related to the number of pores, N_p, and the area of the micrograph, A_m, by,

$$D_{rs} = \sqrt{A_m/N_p} \tag{3}$$

Figure 8 compares the time evolution of the real space domain size, D_{rs}, and light-scattering domain size, D_{ls}, for a 35 wt % solution quenched to 50 °C. The results of two separate real space experiments are shown to confirm the reproducibility and precision of the experimental procedure. The linearity of the data verifies that domain growth is well described by a power law. Also included are data from light scattering showing the rate of growth under identical conditions. The scattering data have been shifted arbitrarily so that they can be

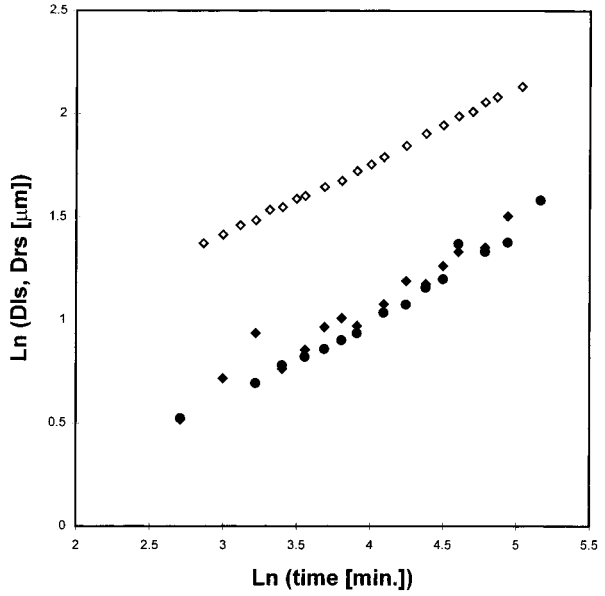

Figure 8. Time dependence of domain size for a 35 wt % solution quenched to 50.0 °C. The closed symbols show the results of two separate real space experiments; the open symbols show light-scattering results.

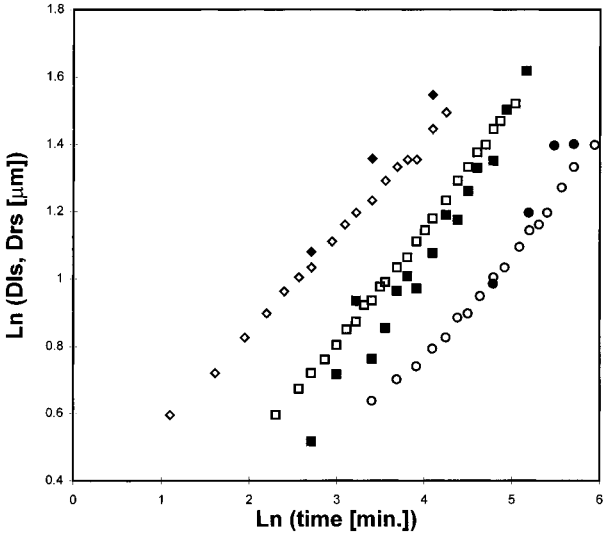

Figure 9. Domain size vs phase separation time for 35 wt % solutions quenched to three temperatures: (●) 47, (■) 50.0, (◆) 54.0 °C. The closed symbols are real space measurements, D_{rs}; the open symbols are scattering measurements, D_{ls}.

easily compared to the real space measurements. The slopes of the two lines are quite close, indicating the correspondence between the light-scattering and real space quantification of the growth rate. In previous studies,[12−16] general trends observed using real space microscopy have been compared to separate light-scattering results of different systems, the implicit assumption being that the exponent determined from real space microscopy is exactly equivalent to that determined by light scattering. Our results provide an experimental justification for such an assumption.

Figure 9 compares light-scattering and real space measurements of 35 wt % solutions quenched to three different temperatures. The temperature-dependent separation of q_m vs time plots has been shown to be independent of cloud point variation.[17] It is therefore reasonable to compare the light-scattering prediction of the separation with the real space measurements. Values of D_{ls} for all of the results shown in Figure 9

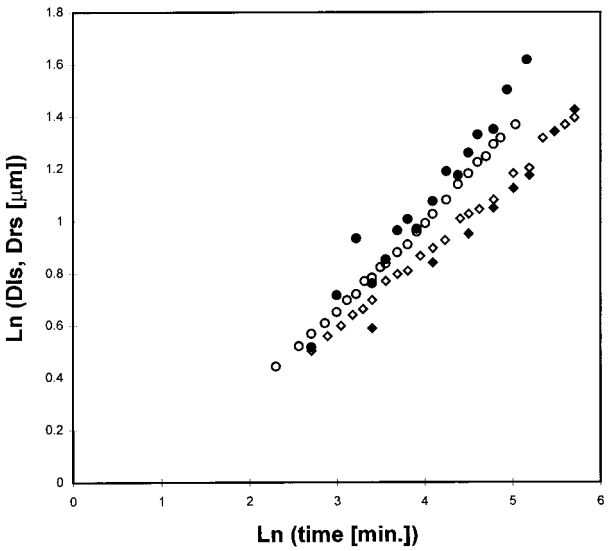

Figure 10. Domain size vs phase separation time for two concentrations, (●) 35 and (♦) 42.5 wt %, quenched to 50.0 °C. The closed symbols are real space measurements; the open symbols are scattering measurements.

have been determined using the proportionality of eq 2 with a constant of 8.15 replacing 2π. Since eq 3 is strictly true only for monodisperse square phases, this agreement can be considered satisfactory. It is apparent from Figure 9 that the temperature-dependent separation of the real space results is well predicted by light-scattering experiments. The results shown in Figure 9 also demonstrate that, for the same annealing time, the domain size decreases with decreasing quench temperature. Consistent with our results, other light-scattering studies of polymer solutions show that the position of the initial intensity maximum increases as the quench temperature is decreased.[5] However, the electron microscopy data of Song and Torkelson[12,13] and the optical microscopy data of McGuire et al.[16] both show the reverse trend. All of the quenches reported in this study were to regions of the phase diagram where the concentrated phase that forms is quite close to its glass transition temperature. As the phase separation temperature is lowered, the polymer-rich phase is expected to be closer to its glass transition temperature where the mobility will be drastically lower. This decrease in mobility is believed to account for the fact that our domains are smaller at the lower phase separation temperatures.

Figure 10 compares light-scattering and real space measurements of 35 and 42.5 wt % solutions quenched to 50 °C. The constant used to calculate D_{ls} was 7, which is slightly lower than that used in Figure 9 because of slight cloud point variation. The results in Figure 10 show that the spacing between light scattering measurements at different concentrations is roughly equivalent to the spacing between the real space measurements. Both light-scattering and real space experiments show that domain size decreases with increasing concentration. This general trend has been observed in several real space studies.[12−14,16]

Conclusions

We have shown that the combination of small-angle light scattering and real space microscopy can be used to quantify the kinetics of two-phase domain growth during thermally induced phase inversion of PMMA/cyclohexanol solutions. The position of the maximum in the small-angle scattering intensity can be used to conveniently monitor the time and temperature dependence of the size scale of the two-phase structure, as well as its arrest due to glass transition. Domain sizes obtained from SEM measurements of annealed, quenched samples show a one-to-one correlation with size scales obtained by light scattering. To our knowledge, ours is the first study demonstrating the quantitative link between arrested phase separation, light scattering, and the size scale of the resultant phase-separated structure.

Acknowledgment. This work has been supported in part by a grant from the National Science Foundation (CTS 94-21580). A.J.P. has also received partial support from the Hauser Scholars Program sponsored by the Chemical Engineering Department.

References and Notes

(1) Castro, A. J. U.S. Patent 4 247 498, Jan 27, 1981.
(2) Caneba, G. T.; Soong, D. S. *Macromolecules* **1985**, *18*, 2538.
(3) Lloyd, D. R.; Kinzer, K. E.; Tseng, H. S. *J. Membr. Sci.* **1990**, *52*, 239.
(4) Lloyd, D. R.; Kin, S. S.; Kinzer, K. E. *J. Membr. Sci.* **1991**, *64*, 1.
(5) Tromp, R. H.; Rennie, A. R.; Jones, R. A. L. *Macromolecules* **1995**, *28*, 4129.
(6) Lal, J.; Bansil, R. *Macromolecules* **1991**, *24*, 290.
(7) Bansil, R.; Lal, J.; Carvalho, B. L. *Polymer* **1992**, *33*, 2961.
(8) Kubota, K.; Kuwahara, N. *Phys. Rev. Lett.* **1992**, *68*, 197.
(9) Kuwahara, N.; Tachikawa, M.; Hamano, K.; Kenmochi, Y. *Phys. Rev. A* **1982**, *25*, 3449.
(10) Kuwahara, N.; Hamano, K.; Aoyama, N.; Nomura, T. *Phys. Rev. A* **1983**, *27*, 1724.
(11) Nojima, S.; Tsutsumi, K.; Nose, T. *Polym. J.* **1982**, *14*, 225.
(12) Song, S.-W.; Torkelson, J. M. *Macromolecules* **1994**, *27*, 6389.
(13) Song, S.-W.; Torkelson, J. M. *J. Membr. Sci.* **1995**, *98*, 209.
(14) Aubert, J. H. *Macromolecules* **1990**, *23*, 1446.
(15) Guo, H.-F.; Laxminarayan, A.; Caneba, G. T.; Solc, K. *J. Appl. Polym. Sci.* **1995**, *55*, 753.
(16) McGuire, K. S.; Laxminarayan, A.; Lloyd, D. R. *Polymer* **1995**, *36*, 4951.
(17) Graham, P. D. Masters Thesis, University of Illinois, Urbana, IL, 1997.
(18) Vandeweerdt, P.; Berghmans, H.; Tervoort, Y. *Macromolecules* **1991**, *24*, 3547.
(19) Cahn, J. W.; Hilliard, J. E. *J. Chem. Phys.* **1958**, *28*, 258.
(20) Cahn, J. W. *J. Chem. Phys.* **1965**, *42*, 93.
(21) Hashimoto, T.; Sasaki, K.; Kawai, H. *Macromolecules* **1984**, *17*, 2812.
(22) Nunes, S. P.; Inoue, T. *J. Membr. Sci.* **1996**, *111*, 93.
(23) Guinier, A. *X-Ray Diffraction*; W. H. Freeman and Co.: San Francisco, 1963.
(24) Lauger, J.; Lay, R.; Maas, S.; Gronski, W. *Macromolecules* **1995**, *28*, 7010.
(25) Binder, K.; Stauffer, D. *Phys. Rev. Lett.* **1974**, *33*, 1006.
(26) Lifshitz, I. M.; Slyozov, V. V. J. *Phys. Chem. Solids* **1961**, *19*, 35.
(27) Burghardt, W. R.; Yilmaz, L.; McHugh, A. J. *Polymer* **1987**, *28*, 2085.
(28) Gaides, G. E.; McHugh, A. J. *Polymer* **1989**, *30*, 2118.

MA961720M